JOURNAL OF GEOPHYSICAL RESEARCH, VOL. 88, NO. B10, PAGES 8160-8170, OCTOBER 10, 1983

THE SHEAR-WAVE VELOCITY GRADIENT AT THE BASE OF THE MANTLE

Thorne Lay and Donald V. Helmberger

Seismological Laboratory, California Institute of Technology

Abstract. The relative amplitudes and travel times of ScS and S phases are utilized to place constraints on the shear-wave velocity gradient above the core-mantle boundary. A previously reported long-period ScSH/SH amplitude ratio minimum in the distance range 65° to 70° is shown to be a localized feature, apparently produced by an amplitude anomaly in the direct S phase, and therefore need not reflect the velocity gradient at the base of the mantle. The amplitude ratios that are free of this anomaly are consistent with calculations for the JB model or models with mild positive or negative velocity gradients in the lowermost 200 km of the mantle. ScSV arrivals are particularly sensitive to the shear velocity structure just above the core-mantle boundary. The apparent arrival time of the peak of ScSV is as much as 4 s greater than that of ScSH in the distance range 75° to 80° for Sea of Okhotsk events recorded in North America. This can be explained by interference effects produced by a localized high velocity layer or strong positive S wave velocity gradient in the lowermost 20 km of the mantle. A velocity increase of about 5% is required to explain the observed shift between ScSV and ScSH. This thin, high velocity layer varies laterally, as it is not observed in similar data from Argentine events. Refined estimates of the outermost core P velocity structure are obtained by modeling SKS signals in the distance range 75° to 85°.

Introduction

The nature of the shear-wave velocity structure at the base of the mantle has been a controversial subject for many years. Gross earth models derived from travel times and free oscillations generally indicate smooth velocity gradients in the lower mantle, with slightly diminished gradients in the lowermost 200 km (D" region). However, these studies have little resolution of the detailed structure of the D" region. Early investigations of diffracted SH waves, relying on classical ray theory interpretations, indicated very low S-wave velocities at the core-mantle boundary (CMB), and attendant strong negative velocity gradients within D" [Cleary et al., 1967; Cleary, 1969; Bolt et al., 1970; Hales and Roberts, 1970; Robinson and Kovach, 1972]. Recent studies of diffracted SH incorporating more complete diffraction theory and synthetic modeling capabilities have proposed milder negative shear velocity gradients in D" [Mondt, 1977; Doornbos and Mondt, 1979] and near-zero or slightly positive gradients [Okal and Geller, 1979; Mula and Müller, 1980; Mula, 1981]. These studies have been directed toward obtaining global averages, and the degree of lateral variation in D" properties remains an open question.

A conflicting result was found by Mitchell and Helmberger [1973], who utilized the relative amplitudes and timing of long-period ScS and S phases to constrain the S-wave velocity gradient in D". They found a minimum in the ScSH/SH amplitude ratio near 68°, which was attributed to low amplitudes of the ScS arrivals. Unable to explain this feature by models with negative or near-zero shear velocity gradients in D", they proposed models with positive S-wave velocity gradients above the CMB. These positive gradients extended over 40 to 70 km above the core, reaching velocities at the CMB as high as 7.6 to 7.8 km/s. These models can explain the observed amplitude ratio behavior, as well as an apparent difference observed in the arrival times of transversely and radially polarized ScS. Mitchell and Helmberger also proposed a low Q_β zone in D", or finite outer core rigidity, to explain the baseline of the ScSH/SH amplitude ratios. While the majority of their data was for deep South American events recorded in North America, they did analyze one deep Sea of Okhotsk event for which the radial and transverse ScS arrival times were not different, which suggested lateral variations in the D" velocity structure.

In this paper we extend the analysis of ScS and S phases using an enlarged data set in order to understand the discrepancy between the diffracted S studies and the results of Mitchell and Helmberger [1973]. A reinterpretation of the ScSH/SH amplitude ratio minimum indicates that this feature is more clearly associated with a localized amplitude anomaly in the direct S waves rather than with D" structure. We find that in general the ScSH amplitude behavior is consistent with the JB model for two distinct lower mantle regions and do not find evidence for a major low Q_β zone at the base of the mantle. ScSV and ScSH do show systematic timing differences for one of the regions, which can be well modeled by introducing a thin high velocity layer or strong positive velocity gradient above the core, but this thin zone varies laterally, and cannot be detected by using the ScSH/SH amplitude ratios alone.

Amplitude Data

The S and ScS data analyzed in this paper are from seven deep focus earthquakes in Argentina and 10 intermediate and deep focus events in the Sea of Okhotsk, recorded at long-period WWSSN and Canadian Seismic Network stations in North America. Figure 1 shows the locations of the stations used for both source regions and the epicenters of the Argentine events. The source parameters for the events are given in Table 1. All of the events were selected for their simple, impulsive waveforms and for their stable SH

Paper number 3B1110.
0148-0227/83/003B-1110$05.00

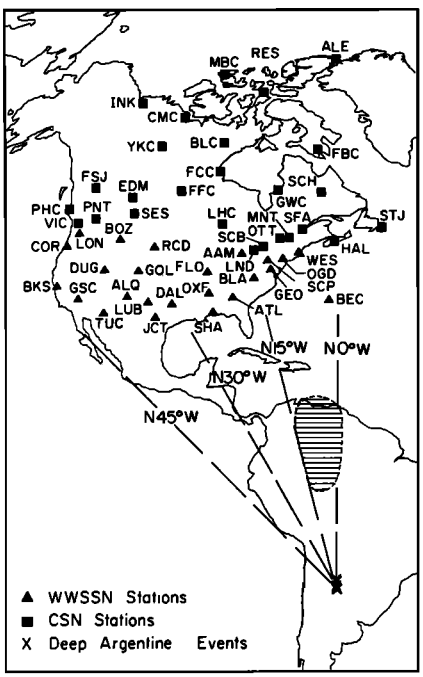

Fig. 1. Azimuthal equidistance projection showing the location of deep Argentine event epicenters and North American stations. GSC, RCD, and SCH are approximately 80° from the Argentine source region. The hatchured region is the map projection of the deep mantle low velocity anomaly proposed by Lay [1983].

radiation patterns to the North American array. The horizontal components in the time interval containing the S and ScS phases of all stations in the distance range 40° to 80° were digitized and rotated into radial and transverse polarizations. A representative profile of the long period tangential component seismograms for one of the Sea of Okhotsk events is shown in Figure 2. For these simple, impulsive waveforms the relative amplitudes and travel times can be accurately measured. Numerous other profiles of the SH seismograms are presented in Lay and Helmberger [1983].

In order to correct the observed amplitudes for radiation pattern, focal mechanisms determined from P wave first motions and S wave polarizations were extracted from the literature or newly determined. Then the long-period SV/SH amplitude ratio was used to refine the mechanisms or to select between various mechanisms in the literature proposed for a given event. This was done by using a modification of a least squares inversion program written by Brian Mitchell. The final focal mechanisms adopted, which are all consistent with both P wave first motions and S wave amplitudes, are listed in Table 2. For the event of July 25, 1969, we could not determine a consistent mechanism. In only four of the 17 cases did we find solutions that significantly improved the SV/SH amplitude agreement over that for the starting mechanisms, and two of these cases involved only 5° changes in dip. This is mainly due to the large scatter in the amplitude ratios.

For the Argentine events, the radiation pattern corrections applied to the observed ScSH/SH amplitude ratios are all less than 12%, which reflects the stability of the SH radiation patterns to North American stations. Since these corrections are small, we include the uncorrected ratios for the event of July 25, 1969, below. Four of the Argentine events in our data set were used by Mitchell and Helmberger [1973]. They applied radiation pattern corrections to their ScSH/SH amplitude ratios that were generally greater than 20% (B. J. Mitchell, personal

TABLE 1. Source Parameters for Events Used in this Study

Date	Origin Time	Latitude	Longitude	Depth, km	Reference
		Sea of Okhotsk			
March 18, 1964	04:37:25.7 ± 0.08	52.56° ± 0.022°N	153.67° ± 0.030°E	424 ± 4.2	ISC
Oct. 12, 1967	12:53:45.9 ± 0.21	52.15° ± 0.018°N	152.57° ± 0.025°E	466 ± 2.7	ISC
Dec. 1, 1967	13:57:02.4	49.5°N	154.4°E	136	NOAA
Sept. 5, 1970	07:52:32.4	52.32°N	151.46°E	583	Strelitz [1975]
Jan. 29, 1971	21:58:06.7	51.72° ± 0.032°N	151.04° ± 0.024°E	540 ± 5.7	Veith [1974]
May 27, 1972	04:06:49.6 ± 0.25	54.97° ± 0.013°N	156.33° ± 0.020°E	397 ± 2.8	ISC
Aug. 21, 1972	06:23:48.6 ± 0.16	49.47° ± 0.012°N	147.08 ± 0.019°E	573 ± 2.2	ISC
July 28, 1973	20:06:35.4 ± 0.15	50.45 ± 0.013°N	148.92 ± 0.022°E	585 ± 2.1	ISC
Sept. 21, 1974	15:54:59.1 ± 0.37	52.19 ± 0.016°N	157.44 ± 0.023°E	119 ± 3.5	ISC
July 10, 1976	11:37:14.0 ± 0.14	47.31 ± 0.011°N	145.75 ± 0.018°E	402 ± 1.7	ISC
		Argentina			
Dec. 9, 1964	13:35:42.4	27.5°S	63.2°W	586	NOAA
Mar. 5, 1965	14:32:19.2	27.0°S	63.3°W	573	NOAA
Dec. 20, 1966	12:26:54.6	26.1°S	63.2°W	586	NOAA
Jan. 17, 1967	01:07:54.3	27.4°S	63.3°W	588	NOAA
Sept. 9, 1967	10:06:44.1	27.7°S	63.1°W	578	NOAA
July 25, 1969	06:06:42.4	25.6°S	63.3°W	579	NOAA
Jan. 3, 1973	02:58:16.7	27.7°S	63.3°W	563	NOAA

communication, 1982). The focal mechanisms they used were also determined using SV/SH amplitudes but in some cases were inconsistent with the P-wave first motions. The scatter in the amplitudes is substantial, and probably the larger size of our data sets for each event provides more reliable mechanisms.

The long-period peak-to-peak ScSH/SH amplitude ratios for the Argentine data are shown in Figure 3. Radiation pattern corrections have been applied. In the distance range 55° to 75° the S and ScS arrivals are distinct phases for which the amplitudes can be accurately measured. Beyond 75°, ScS interferes with the instrument

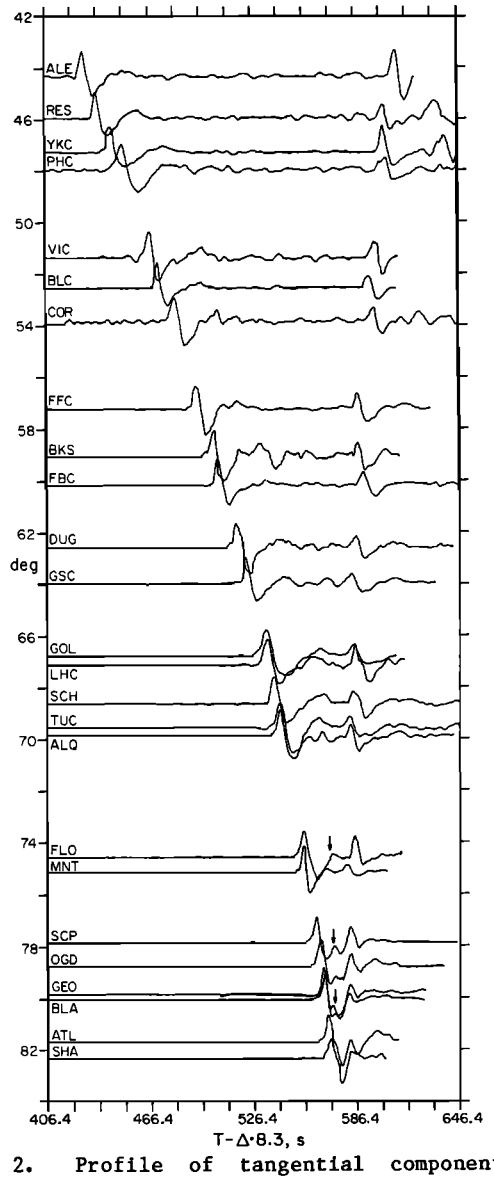

Fig. 2. Profile of tangential components at North American stations for the September 5, 1970, Sea of Okhotsk event (d = 583 km). Direct S is the first large arrival in each trace with ScS arriving around 580-600 s. Station JB travel time anomalies have been removed, and the amplitudes are normalized. The arrows indicate the arrival of an ScS precursor produced by the triplication discussed by Lay and Helmberger [1983].

TABLE 2. Fault Plane Orientations

Date	Strike, degree	Dip, degree	Rake, degree
Dec. 9, 1964	171	78	-90
March 5, 1965	12	26	-68
Dec. 20, 1966	30	43	-42
Jan. 17, 1967	28	30	-44
Sept. 9, 1967	3	19	-78
Jan. 3, 1973	357	28	-83
March 18, 1964	48	84	-76
Oct. 12, 1967	30	75	-52
Dec. 1, 1967	50	87	109
Sept. 5, 1970	12	74	-77
Jan. 29, 1971	40	77	-119
May 27, 1972	25	82	-93
Aug. 21, 1972	18	19	44
July 28, 1973	51	76	-107
Sept. 21, 1974	205	79	80
July 10, 1976	40	81	-87

overshoot of the direct S arrival, and the apparent peak-to-peak amplitude of ScS diminishes rapidly. There is a factor of 3 scatter at each distance, which complicates the interpretation of the amplitude ratios. This scatter is primarily due to source and receiver structure complexity as well as deep mantle structure.

Figure 3 also shows the theoretical ScSH/SH amplitude ratio for a JB earth model. The curve was determined from long-period synthetics computed by using the Cagniard de Hoop generalized ray theory technique [see Lay and Helmberger, 1983]. The effective t_β^* is the same for S and ScS for this and all other synthetic calculations presented here. For a lower mantle with a constant Q_β = 312 (e.g., the PREM model of Dziewonski and Anderson [1981]) the difference in t_β^* for ScS and S varies from 0.2 to 0.0 s in the distance range 55° to 80°, which produces an insignificant effect on the long-period amplitude ratios. However, for a model with a very low Q_β distribution near the CMB such as model SL8 [Anderson and Hart, 1978], the difference in t_β^* increases from 0.25 to 1.0 s in the same distance range, which predicts a more rapid decay in the ScSH/SH amplitude ratios with distance than is apparent in the theoretical curve in Figure 3.

The data in Figure 3 can be compared with that in Figure 6 of Mitchell and Helmberger [1973] if one omits their data points for Peruvian events and the Sea of Okhotsk event. Figure 3 has twice as many data points for the Argentine source region. In the range 65° to 70° there is a cluster of low amplitude ratios, well below the JB model calculations, but there are numerous observations in this range consistent with the JB model. At distances greater than 75° the observed ratios drop off rapidly due to the interference between S and ScS, and the theoretical curve does also since the long-period synthetics have similar interference. As is shown later, similar data from the Sea of Okhotsk source region do not show an amplitude minimum near 67°, so this anomaly is investigated in detail below. It is also important to note that the amplitude ratios in Figure 3 scatter in the range 0.2 to 0.75, which is significantly shifted

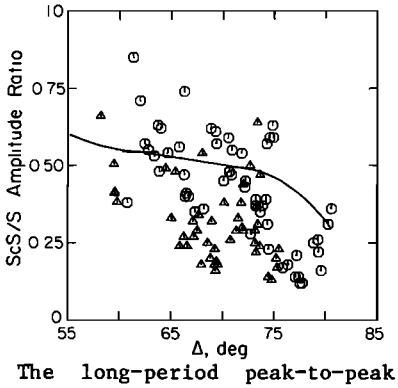

Fig. 3. The long-period peak-to-peak ScSH/SH amplitude ratios for the Argentine events recorded in North America. Radiation pattern corrections for the focal mechanisms given in Table 2 have been applied. The triangles are for data recorded at azimuths to the east of N15°W from the source region. The curve shows the theoretical ratios measured from long-period synthetics for the JB model.

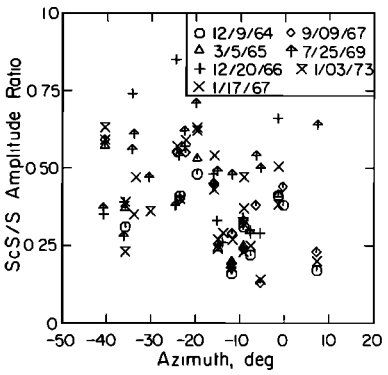

Fig. 4. The same data in Figure 3 plotted as a function of azimuth from the source. Different symbols are used for each event. Only data in the distance range 55° to 75° are shown, because the expected distance dependence is small in this range.

relative to the range 0.1 to 0.5 spanned by the data in Mitchell and Helmberger [1973]. This shift, which apparently results from the difference in radiation pattern corrections applied, is important because the low average baseline of the data in the earlier study was cited as evidence for a low Q_β region at the base of the mantle.

A close inspection of the individual observations that define the amplitude ratio minimum near 67° in our Figure 3 and Figure 6 of Mitchell and Helmberger [1973] reveals that all of the stations involved lie on the east coast of North America. In particular, SCP, OGD, BLA, GEO, LND, MNT, OTT, and SFA (Figure 1) repeatedly have low amplitude ratios. Stations at comparable distance such as OXF, FLO, and LUB do not show low amplitude ratios. This indicates an azimuthally restricted anomaly, which probably does not reflect radial earth structure. In Figure 3 all of the observations at azimuths from the source region east of N15°W are plotted with triangles. There is relatively little overlap between the two populations for this azimuthal separation, and all of the anomalously low ratios are isolated to eastern observations.

The Argentine ScSH/SH amplitude ratios are plotted as a function of azimuth in Figure 4. The sharp separation of the low ratios along an azimuth of N15°W indicates the localized nature of the amplitude anomaly. The event of July 25, 1969, shows some relatively large amplitude ratios at eastern stations, but these may be erroneous because radiation pattern corrections were not applied for that event. The data at an azimuth of 0° are for station BEC, which is near 55° distance. This station is isolated from the east coast (Figure 1) and appears to be free of the azimuthal anomaly.

The amplitude ratio minimum could result from either an S or ScS amplitude anomaly. Mitchell and Helmberger [1973] inferred that the ScS phases were responsible based on the distance behavior of S and ScS amplitudes. In Figure 5 the zero line-to-first peak amplitudes for S and ScS are plotted as a function of azimuth. Geometric spreading corrections determined from synthetics for a JB mantle have been applied, along with radiation pattern and event size corrections. The S waves show an azimuthal pattern, with relatively high amplitudes recorded at east coast stations. There is no corresponding trend in the ScS data. The factor of 2 to 3 enhancement of the S amplitudes in the east can account for the ScSH/SH amplitude anomaly. Lay [1983] compared the long-period SH amplitude anomalies at North American stations for the Argentine and Sea of Okhotsk source regions. The Argentine data generally show relative enhancement of the SH amplitudes at east coast stations, which indicates that the trend in Figure 5 is not due to receiver structure.

Further evidence that the SH waves from Argentina are anomalous is given by Lay [1983], who studied the travel times from this data set. He concluded that the SH waves are 2 to 5 s late at the east coast stations and that this is

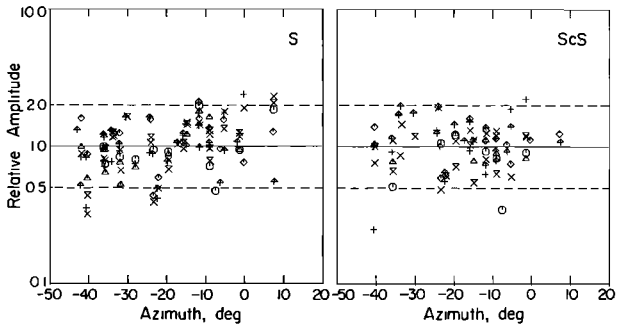

Fig. 5. The long period first peak SH (left) and ScSH (right) amplitudes from the Argentine events plotted as a function of azimuth from the source. Radiation pattern and geometrical spreading corrections have been applied as well as event size corrections. Note the relatively high S amplitudes recorded at east coast station, whereas the ScS amplitudes at these stations are not enhanced. The symbols are the same as in Figure 4. ScS amplitudes at distances greater than 75° are not included.

because they encounter an anomalously low velocity region in the lower mantle at depths of 1700 to 2700 km. The ScS times at these stations are not anomalous, nor are the S or ScS times at BEC. The map projection of this lower mantle anomaly is shown in Figure 1.

Since the data recorded at east coast stations appears to be contaminated by an anomaly in the direct S phase, we have removed the east coast observations from the Argentine data set in Figure 6. The observations at BEC were retained since they are free of any obvious travel time or amplitude anomaly. As was discussed in Lay [1983], there may be an additional S wave amplitude anomaly in the midwestern and southern stations, with diminished S amplitudes producing large ScS/S ratios. This is not as well established as the east coast anomaly, but it should be kept in mind that some of the larger values in Figure 6 may be due to structure along the S-wave path. The JB model provides a reasonable fit to the average amplitude ratio behavior, throughout the range 55° to 75°, and there is no clear fine structure requiring lower mantle complexity. The average observed amplitude ratio level is generally compatible with the calculations for which t^*_β is the same for S and ScS, which indicates that no low Q_β zone at the base of the mantle is required by this data. Note that even if some of the ScS/S amplitude anomaly at the east coast stations is due to the ScS phases, despite the evidence presented above to the contrary, it is still clear that the anomaly is azimuthally restricted, and no radial earth structure can account for it.

We have computed the theoretical ScSH/SH amplitude ratios as a function of distance for modified JB models with positive and negative linear velocity profiles in D". The dashed lines in Figure 6 indicate the envelope of the theoretical ratios for all models with constant gradients over 20 to 200 km thick zones with velocities at the CMB ranging from 7.0 to 7.6 km/s (7.3 km/s for the JB model). Models with stronger velocity increases produce large ScS

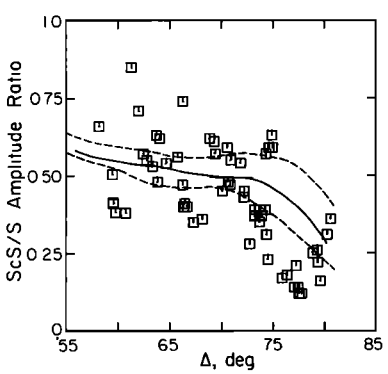

Fig. 6. The long-period peak-to-peak ScSH/SH amplitude ratios for the Argentine events recorded in North America at azimuths to the west of N15°W from the source, as well as at BEC. The solid curve shows the theoretical ratios for the JB model. The dashed curves indicate the envelope of amplitude ratios for models with mild positive and negative velocity gradients above the core. Details are given in the text.

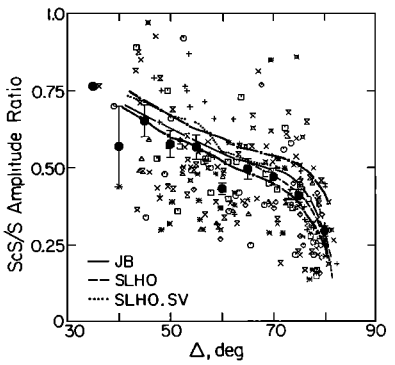

Fig. 7. The long-period peak-to-peak ScS/S amplitude ratio for Sea of Okhotsk observations in North America. Different symbols correspond to different events. The solid symbols give the mean and standard error of the observations in each 5° increment of distance. At distances greater than 75° the amplitude ratio is contaminated by interference between S and ScS. The labeled curves are theoretical ratios measured from synthetics for the models discussed in the text. The dash-dot curves indicate the envelope of theoretical ratios for the models with mild positive and negative linear gradients in D" discussed in the text.

amplitudes around 75° which are inconsistent with the data. Thin (<60 km) negative gradient transition zones reaching velocities less than 7.0 km/s produce a precursor to ScS which is not observed, so these models can also be ruled out. The individual models produce fine structure in the ScSH/SH amplitude ratios not apparent in the JB model calculations, but the data scatter too much to resolve any such features. At distances beyond 75° the theoretical computations scatter more because of the variable interference between S and ScS, and little constraint on the velocity structure can be inferred.

Lay and Helmberger [1983] have shown that an S-wave triplication in the Argentine and Sea of Okhotsk data indicates the presence of a 2.75% shear-velocity discontinuity 250 to 280 km above the CMB. The presence of this structure does not strongly affect the ScSH/SH amplitude ratios, so the results found here by using the JB model as a reference mantle structure apply to models with a discontinuity at the top of D" as well.

In Figure 7 the long-period ScSH/SH amplitude ratios for the 10 Sea of Okhotsk events recorded in North America are shown as a function of distance. The amplitude ratios are corrected for radiation pattern. The source parameters and focal mechanisms for these events are given in in Tables 1 and 2. The data appear to be free of any large-scale azimuthal anomalies in the travel times or amplitudes. The region of D" sampled lies below Alaska and western Canada. There is again a large amount of scatter, but the observations are numerous enough to compute meaningful averages in each 5° increment of distance, as shown. The data are reliable to a distance of 75°, beyond which the ScS phases interfere with the arrivals of the lower mantle triplication [Lay and Helmberger, 1983].

As for the Argentine data, the JB model

produces a reasonable fit to the average ScSH/SH observations. The slight minimum observed near 60° may be resolvable but is not a prominent feature. While many data points lie below the JB predictions, there is no compelling evidence for a low Q_β region in D" for this path. The dash-dot curves indicate the same range in theoretical amplitude ratios as shown in Figure 6 and discussed above. These are consistent with the data averages in the range 40° to 75°. None of the constant gradient models investigated produce a localized minimum near 60°. Model SLHO (see Figure 10) is a structure with a 2.75% S-wave velocity discontinuity 278 km above the CMB determined for this path by Lay and Helmberger [1983]. The velocity gradient in D" is slightly positive for this model, and the predicted ScSH/SH ratios are practically indistinguishable from those of the JB model. Model SLHO.SV, which is derived below, is similar to SLHO but has a 20 km thick high velocity (7.6 km/s) layer just above the core. This sharp velocity increase produces little effect on the long-period ScSH/SH ratios, which indicates the insensitivity of the SH phases to thin regions of high velocity gradient near the CMB. Clearly, the long-period ScSH/SH amplitude ratios do not uniquely constrain the shear-velocity gradient in D". Short-period data may help greatly and will be analyzed in a future paper. The data are consistent with the JB model or with models with slightly positive or negative gradients in D".

ScSV-ScSH Travel Time Data

Mitchell and Helmberger [1973] suggested that comparison of the arrival time of long-period ScSV and ScSH can be used to determine the shear-velocity gradient just above the core. They found that in the range 60° to 75° the peak of ScSV arrives progressively later than the peak of ScSH for the Argentine data. This shift was attributed to an interference effect produced by ScS precursors reflected from a positive velocity gradient at the base of D". Such a gradient produces a reflection in phase with ScSH and out of phase with ScSV, which causes a relative shift in the peak arrival of the core reflection on long-period records.

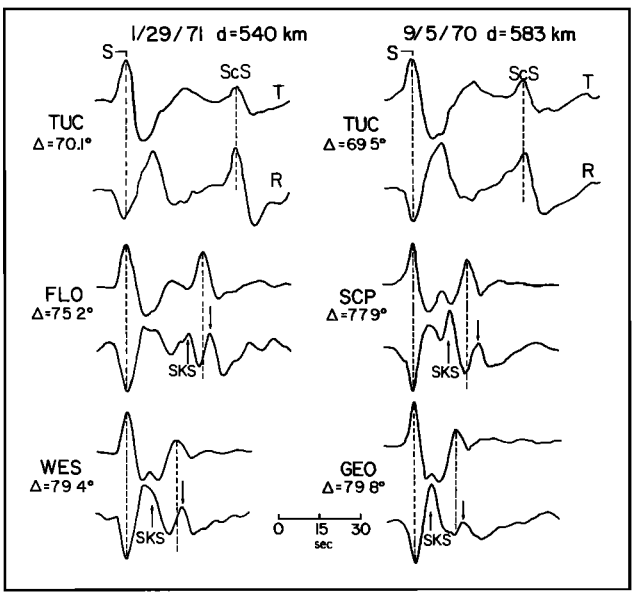

Fig. 8. Comparison of tangential (T) and radial (R) components of two deep focus Sea of Okhotsk events recorded in North America. The SH and SV peak amplitudes arrive at the same time at all distances. ScSV and ScSH arrive at the same time near 70°. Beyond 70°, the apparent ScSV arrival (↓) is shifted later than the ScSH arrival. This is not explained simply by the interference of SKS (↑) on the radial component.

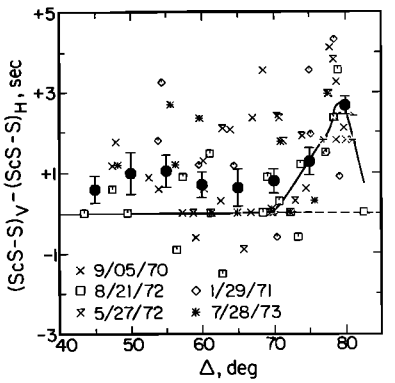

Fig. 9. Observed differences in ScS-S differential times measured peak-to-peak on the long-period radial and tangential components for the Sea of Okhotsk observations in North America. The solid symbols give the mean and standard error of the observations in each 5° increment in distance. The solid curve is for model SLHO.SV.

In our data set the SV signals are often nodal at the North American stations, but enough reliable observations could be made to test the relative ScS timing. If one compares the ScSH and ScSV arrivals for the Sea of Okhotsk data, it is found that beyond 75°, the apparent ScSV arrival is late relative to ScSH. This is demonstrated in Figure 8. Noting that the ScS arrival should have upward motion in the figure for both components, it is clear that the peak of the ScSV component is shifted by as much as 4 s relative to the peak of ScSH. The direct S pulses show no corresponding shift. Since the SKS arrival pulls ahead of ScSV beyond 70°, one might attribute this shift to the interference between the downswing of the SKS arrival and the ScSV upswing. However, the ScSV shift is still observed at 80° where SKS is relatively far ahead of ScSV. Furthermore, when we compute SV synthetics including the SKS arrival, no differential shift in the peak of ScSV relative to that of ScSH is observed, as shown below.

The peak-to-peak ScS-S differential times on the radial and tangential components were measured for all of the Sea of Okhotsk data for which the phases are fairly clear on both components at North American stations. Since measurement of the ScSV timing is ambiguous at distances greater than 75° due to the SKS arrival, we measured the arrival time of the ScSV "peaks" indicated in Figure 8. These peaks clearly reflect an interference effect, but they have a stable behavior which can be reliably compared with times that are similarly measured from synthetics with corresponding interference effects. The difference in these differential

times is plotted against distance in Figure 9, along with the average and standard error of the observations in each 5° increment of distance. While, on average, there is a slight positive residual at all distances, which is difficult to explain as a structural effect, there is a clear increase in the differential measurement beyond 70°. Since the peaks of the direct arrivals are found to be at the same time in almost all cases, this difference is basically a measure of the apparent ScSV-ScSH difference produced by different interference effects on the radial and transverse components. The large number of observations indicates the robustness of this anomaly. The distance dependence of this observation suggests that it results from velocity structure rather than anisotropy or lateral variations in D". We have, therefore, sought to explain the observation by introducing fine velocity structure into the D" region. Following the reasoning of Mitchell and Helmberger [1973], it is possible to produce this apparent shift in ScSV relative to ScSH by producing an interfering arrival just ahead of the core reflection. A strong positive velocity gradient or discontinuity can accomplish this as suggested above.

Through trial-and-error waveform modeling we have obtained a modified SLHO model which satisfies both SH and SV observations from the Sea of Okhotsk recorded in North America. This model, SLHO.SV, is presented in Figure 10. The major modification of SLHO is the introduction of a thin high velocity layer 20 km thick at the base of D". This layer produces a strong post-critical reflection which interferes with ScSH constructively and a negative reflection which interferes with ScSV destructively producing a relative shift in the peak arrival time of ScSV. The velocity increase must be on the order of 5% in order to produce as much as 3 s shifts in the peak of ScSV. The differential ScSV-ScSH travel times measured from synthetic seismograms for this model are plotted in Figure 9. These fit the average data well, though the largest anomalies are a full second greater than even SLHO.SV predicts. Beyond 80° the post-critical reflection weakens, and the interference producing the ScSV shift diminishes.

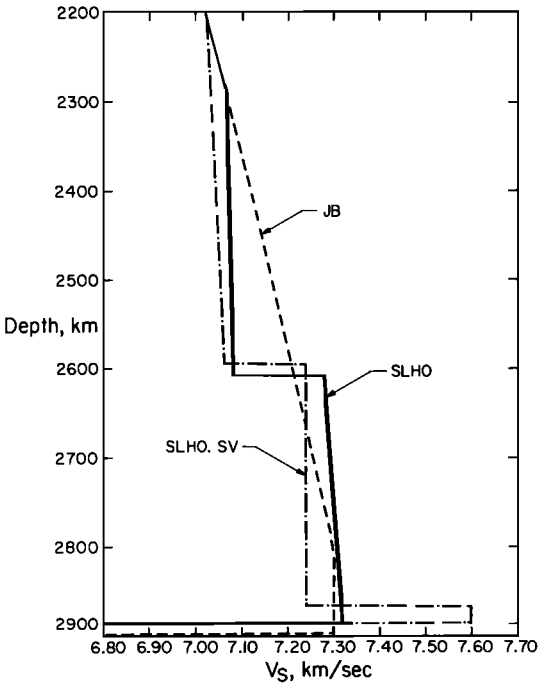

Fig. 10. Comparison of the JB reference model and models SLHO and SLHO.SV. SLHO provides a good fit to the SH data alone, and SLHO.SV fits both SH and SV, for the Sea of Okhotsk events recorded in North America.

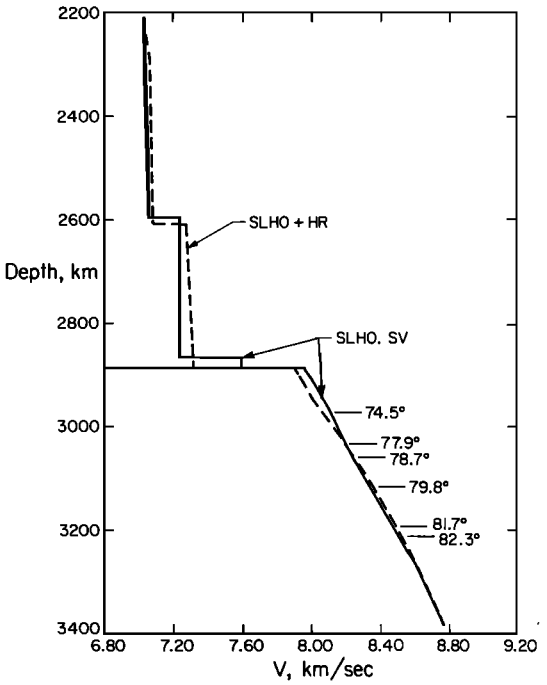

Fig. 11. Comparison of the starting (SLHO + HR) and final (SLHO.SV) models for the S structure of the lower mantle and P wave structure of the outer core for paths from the Sea of Okhotsk to North America. The starting core model is from Hales and Roberts [1971]. The bottoming depths for the SKS arrivals in the SLHO.SV synthetics in Figure 12 are indicated by the distances.

In the course of modeling the SV seismograms, it was necessary to adopt a core model that predicts the correct SKS timing and amplitude. We measured the differential times of SKS-S for all the Okhotsk observations and found that these times were on average 4 s greater than for the JB model and only 1 s slower than for the Hales and Roberts [1971] model. Since the primary difference between these two models affecting SKS-S times is the lower velocities in the outermost core of the Hales and Roberts (HR) model, we adopted their core velocity structure as a starting model. Combining this model with SLHO produces excellent SKS-S travel time agreement with the data throughout the range 70°-83°. In determining the SLHO.SV model it was necessary to adjust simultaneously the core velocities in the outermost 100 km of the core. Figure 11 shows the starting SLHO and HR model and the final SLHO.SV model. The depths at which SKS bottoms in the outer core for various distances are indicated. Note that the modified core model of SLHO.SV has a somewhat smoother gradient in the outer 300 km of the core than the

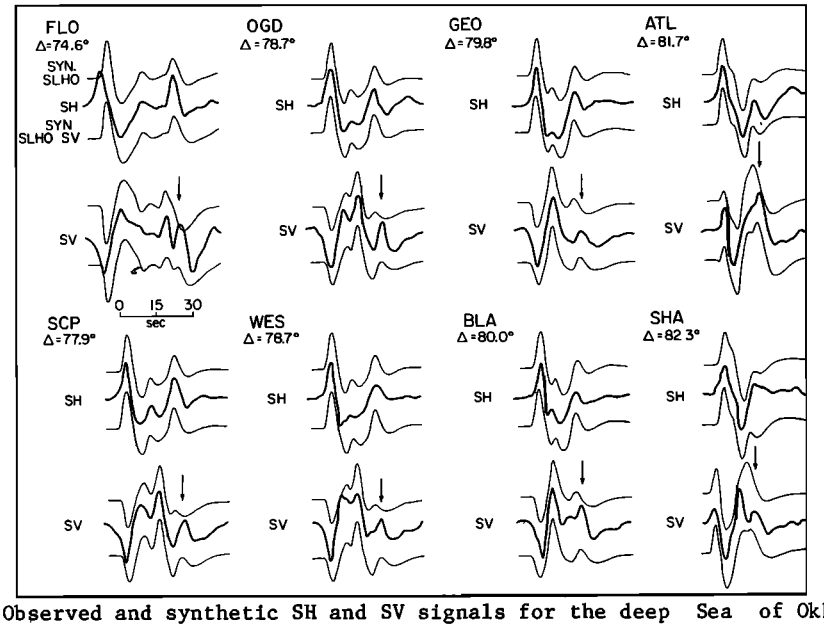

Fig. 12. Observed and synthetic SH and SV signals for the deep Sea of Okhotsk event of September 5, 1970. The top synthetic in each trace is for model SLHO overlying a Hales and Roberts [1971] core model. The lower synthetic is for model SLHO.SV (Figure 11) overlying a modified core model. Both models fit the SH observations well, but for model SLHO the ScSV portion of the waveform (↓) is not accurately modeled. The interference caused by the high velocity layer in model SLHO.SV fits the entire SV waveform.

Hales and Roberts model, which is consistent with most other core models. This change in gradient can be resolved in the data by comparing ScSV and SKS at distances less than 75°. Modeling additional direct SKS data in this distance range promises to yield exceptional resolution of the outermost core velocities, which can otherwise only be roughly obtained by using SK_nS multiples.

Model SLHO.SV was determined not only by fitting the differential travel time of ScSV but by fitting the entire SH and SV waveforms. In Figure 12, observed SH and SV signals are compared with ray theory synthetics for the SLHO and HR model (top trace in each comparison). While SLHO fits all of the SH signal and the SV data are adequately modeled through the SKS arrival, at each station the peak ScSV signal is too early in all of the synthetics for this model. Note that the upward peaks produced by the ScSV arrival are not shifted relative to those produced by ScSH. This proves true for any shear velocity model with flat gradients above the CMB. The synthetics for model SLHO.SV (bottom trace in each comparison) are equally good for the SH signals, with only slight discernable differences from the SLHO synthetics. However, now the entire SV waveform is well modeled, including the splitting of the SKS and ScSV signals at FLO and the long period ScSV coda at WES, GEO, and SCP. In generating the synthetics for model SLHO.SV the first three multiple S bounces within the high velocity layer have been included. The lack of sensitivity of the SH data to a thin high velocity region is a bit surprising and indicates the insensitivity of the ScSH/SH amplitude ratio for modeling D" velocity structure. The synthetic SH amplitude ratios for SLHO.SV are included in Figure 7, which shows that the SH amplitude data are quite consistent with model SLHO.SV.

The synthetic SV waveform improvement is quite substantial for model SLHO.SV; however, we feel that additional data must be obtained before a definitive model can be determined. In particular, the thickness and velocity contrast of the high velocity layer in model SLHO.SV are not uniquely constrained. The SV waveforms in the range 75°-85° represent a complicated interference pattern between SK_nS, SVab, SVcd (where ab and cd indicate the branches of the lower mantle triplication caused by the discontinuity at the top of D"), and ScSV, and one must be cautious in interpreting this complexity. However, it does appear that localized strong positive velocity gradients exist in the D" region.

For most of the Argentine events the SV signals are nodal; however, there are enough observations with stable SH and SV signals to make a comparison of the ScSV and ScSH arrivals. Mitchell and Helmberger [1973] previously reported a systematic increase in the apparent ScSV-ScSH arrival time difference for the Argentine data in the range 65° to 75°. Our data set is shown in Figure 13, with the number of Argentine observations being about twice that shown by Mitchell and Helmberger [1973]. While there is a slight increase in the differential times near 75°, there is no trend comparable to that in the Sea of Okhotsk data shown in Figure 9. Near 75° it is difficult to time ScSV because SKS arrives just a few seconds ahead, and near 80° it is difficult to identify the ScS arrival, but there is no indication of an interference effect. We feel that these data do not indicate the presence of a strong positive velocity

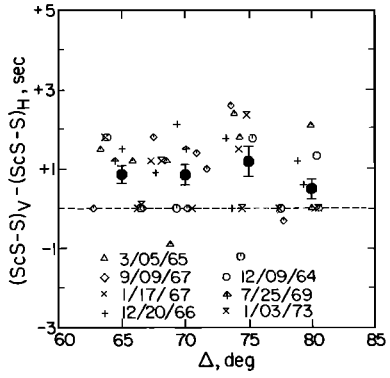

Fig. 13. Observed differences in ScS-S differential times measured peak-to-peak on the radial and tangential components for Argentine observations in North America. The solid symbols give the mean and standard error of the observations in each 5° increment in distance.

increase like that sampled by the path from the Sea of Okhotsk to North America. Therefore, it appears that the high velocity layer producing the interference varies laterally.

It is desirable to check the SH synthetics generated by the Cagniard de Hoop method by comparing them with the reflectivity method developed by Fuchs and Müller [1971] and Kind and Müller [1975]. The effect of multiple bounces within the high velocity layer in model SLHO.SV is particularly important to assess. Figure 14 compares synthetic profiles for the two methods for a source depth of 580 km and no Q structure.

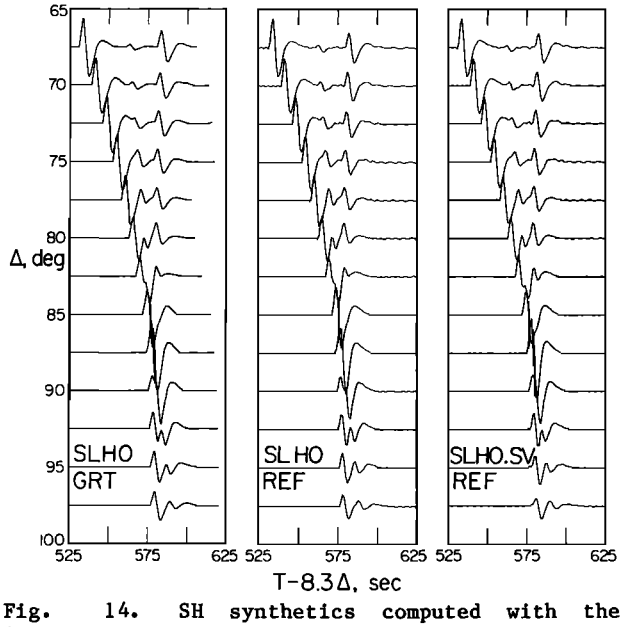

Fig. 14. SH synthetics computed with the Cagniard de Hoop generalized ray theory (GRT) technique and the reflectivity (REF) technique for the Sea of Okhotsk models. The agreement between these techniques throughout the entire range of the lower mantle triplication is clearly apparent. The introduction of the thin high velocity layer in model SLHO.SV does not strongly affect the SH signals.

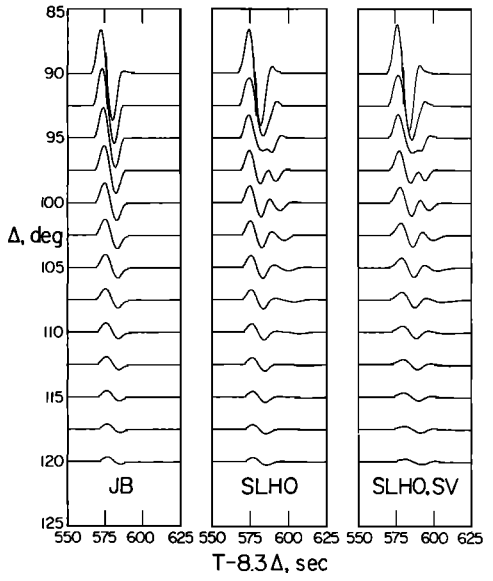

Fig. 15. SH synthetics for the JB and Sea of Okhotsk models shown in Figure 10. The reflectivity technique was used to compute the signals. The amplitude scale is the same for all three models. The presence of the receding Sab branch causes the distortion in the range 95° to 100° for models SLHO and SLHO.SV. The diffracted signals, beyond 105°, are very similar for the three models, with little discernable difference in waveform character. The high velocity layer in SLHO.SV causes a more rapid amplitude decay of diffracted S than in the other models.

The generalized ray theory (GRT) and reflectivity synthetics for model SLHO are almost indistinguishable from those for model SLHO.SV. This comparison indicates that the ray theory synthetics are reliable for this application.

Figure 15 shows reflectivity synthetics for diffracted SH for the JB model and the two Sea of Okhotsk models. The source wavelet has a dominant period of 20 s, which is comparable to that of long period diffracted SH observations at WWSSN stations. In the range 95° to 100° the Sab branch, which corresponds to energy traveling along the discontinuity at the top of D", produces a secondary arrival which diminishes rather quickly. For model SLHO.SV the amplitude decay into the shadow region is more rapid than for the JB and SLHO models. Depending on the extent of the high velocity layer, it may or may not be possible to detect this subtle difference by analyzing diffracted SH waves.

Discussion

The ScSH data presented in this paper do not provide tight constraints on the D" shear-velocity structure, owing to both the large amount of scatter in the amplitude data and the intrinsic lack of sensitivity to fine velocity structure of the long-period phases. However, the amplitude data do not clearly require major deviations from the smoothly varying velocity gradients in D" of the JB model. Analysis of diffracted phases and short-period signals may

provide higher resolution of the shear-velocity gradients above the core; however, future efforts must concentrate on regional variations more than previous work. Future studies must also place greater emphasis on eliminating the spectral contamination caused by complex receiver structures [Lay and Helmberger, 1981] before spectral analysis of diffracted waves and short periods will yield high resolution of lower mantle structure. Lay and Helmberger [1983] show that there are resolvable lateral variations in the velocity structure at the top of D". The ScSV-ScSH differential travel times shown here indicate lateral variations in the fine structure at the base of D" as well. The thin high velocity region at the base of the mantle detected in the Sea of Okhotsk data does appear to vary laterally, as might be expected for such a thin, anomalous layer. Possibly this layer represents a localized compositional heterogeneity. Such a feature may serve as the type of scatterer often attributed to the D" region [e.g., King et al., 1973; Haddon and Cleary, 1973].

While this paper has reassessed the data and interpretations presented by Mitchell and Helmberger [1973], and yields very different results, their basic approach to the data remains sound. ScS phases sample very localized portions of the D" region, which provides an opportunity to study lateral variations in the region obscured in travel time or diffracted wave studies. It is important to exercise caution when interpreting differential times and relative amplitudes because of the accumulating evidence for large velocity and amplitude anomalies produced by deep source region structure and localized anomalies in the central part of the lower mantle [Jordan, 1977; Lay, 1983].

Conclusions

An analysis of long-period ScS amplitude behavior indicates that the JB model or models with mild positive or negative velocity gradients above the core-mantle boundary are consistent with data for two distinct regions of D". An ScSH/SH amplitude ratio minimum reported by Mitchell and Helmberger [1973] appears to result from anomalous S amplitudes rather than from D" structure and is an azimuthally restricted anomaly. The long-period ScS amplitudes do not give any clear indication of a very low Q_β zone at the base of the mantle. A systematic distance trend in the difference of the peak arrival times of ScSH and ScSV for paths below Alaska indicates the presence of a localized high velocity gradient just above the core. This structure appears to vary laterally, for data from South American earthquakes do not show a similar trend. A refined outer core P wave velocity model is determined by modeling SKS signals in the range 75° to 85°.

Acknowledgments. Don Anderson and Terry Wallace reviewed the manuscript and provided helpful suggestions. We thank Brian Mitchell for providing us with his version of the SV/SH amplitude inversion program and comments on his data. We thank Gerhardt Müller for providing us with a copy of the SH reflectivity program written by Wolfgang Schott. This research was supported in part by the National Science Foundation under grant NSF EAR 810-8616. Contribution number 3837, Division of Geological and Planetary Sciences, California Institute of Technology.

References

Anderson, D. L., and R. S. Hart, Q of the earth, J. Geophys. Res., 83, 5869-5882, 1978.

Bolt, B. A., M. Niazi, and M. R. Somerville, Diffracted ScS and the shear velocity at the core boundary, Geophys. J. R. Astron. Soc., 19, 299-305, 1970.

Cleary, J., The S velocity at the core-mantle boundary, from observations of diffracted S, Bull. Seismol. Soc. Am., 59, 1399-1405, 1969.

Cleary, J., K. Porra, and L. Reed, Diffracted S, Nature, 216, 905-906, 1967.

Doornbos, D. J., and J. C. Mondt, P and S waves diffracted around the core and the velocity structure at the base of the mantle, Geophys. J. R. Astron. Soc., 57, 381-395, 1979.

Dziewonski, A. M., and D. L. Anderson, Preliminary reference earth model, Phys. Earth Planet. Interiors, 25, 297-356, 1981.

Fuchs, K., and G. Müller, Computation of synthetic seismograms with the reflectivity method and comparison with observations, Geophys. J. R. Astron. Soc., 23, 417-433, 1971.

Haddon, R. A. W., and J. R. Cleary, Evidence for scattering of seismic PKP waves near the mantle-core boundary, Phys. Earth Planet. Interiors, 8, 211-234, 1973.

Hales, A. L., and J. L. Roberts, The travel times of S and SKS, Bull. Seismol. Soc. Am., 60, 461-489, 1970.

Hales, A. L., and J. L. Roberts, The velocities in the outer core, Bull. Seismol. Soc. Am., 61, 1051-1059, 1971.

Jordan, T., Lithospheric slab penetration into the lower mantle beneath the Sea of Okhotsk, J. Geophys., 43, 473-496, 1977.

Kind, R., and G. Müller, Computations of SV waves in realistic earth models, J. Geophys., 41, 149-175, 1975.

King, D. W., R. A. W. Haddon, and J. R. Cleary, Evidence for seismic wave scattering in the D" layer, Earth Planet. Sci. Lett., 20, 353-356, 1973.

Lay, T., Localized velocity anomalies in the lower mantle, Geophys. J. R. Astron. Soc., 72, 483-516, 1983.

Lay, T., and D. V. Helmberger, Body wave amplitude patterns and upper mantle attenuation variations across North America, Geophys. J. R. Astron. Soc., 66, 691-726, 1981.

Lay, T., and D. V. Helmberger, A lower mantle S wave triplication and the shear velocity structure of D", Geophys. J. R. Astron. Soc., in press, 1983.

Mitchell, B. J., and D. V. Helmberger, Shear velocities at the base of the mantle from observations of S and ScS, J. Geophys. Res., 78, 6009-6020, 1973.

Mondt, J. C., SH waves: Theory and observations

for epicentral distances greater than 90 degrees, Phys. Earth Planet. Interiors, 15, 46-59, 1977.

Mula, A. H. G., Amplitudes of diffracted long-period P and S waves and the velocities and Q structure at the base of the mantle, J. Geophys. Res., 86, 4999-5011, 1981.

Mula, A. H., and G. Müller, Ray parameters of diffracted long-period P and S waves and the velocities at the base of the mantle, Pure Appl. Geophys., 118, 1272-1292, 1980.

Okal, E. A., and R. J. Geller, Shear-wave velocity at the base of the mantle from profiles of diffracted SH waves, Bull. Seismol. Soc. Am., 69, 1039-1053, 1979.

Robinson, R., and R. L. Kovach, Shear wave velocities in the earth's mantle, Phys. Earth Planet. Interiors, 5, 30-44, 1972.

Strelitz, R., The September 5, 1970 Sea of Okhotsk earthquake: A multiple event with evidence of triggering, Geophys. Res. Lett., 2, 124-127, 1975.

Veith, K. F., The relationship of island arc seismicity to plate tectonics, Ph.D. Thesis, Southern Methodist University, Dallas, Texas, 1974.

D. V. Helmberger and T. Lay, Seismological Laboratory, California Institute of Technology, Pasadena, CA 91125.

(Received October 14, 1982;
revised June 3, 1983;
accepted June 27, 1983.)